A comparison of repetitive corrugation and straightening and high-pressure torsion using an Al-Mg-Sc alloy

Prabhakar M. Bhovi[1], Deepak C. Patil[2], S. A. Kori[3], K. Venkateswarlu[4,*], Yi Huang[5,*], Terence G. Langdon[5]

[1]B.V. Bhoomaraddi College of Engineering and Technology, Hubballi-580031, India
[2]KLE Dr.M.S. Sheshgiri College of Engineering and Technology, Belagavi-590008, India
[3] Basaveshwar Engineering College, Bagalkot-587102, Karnataka, India
[4]CSIR-National Aerospace Laboratories, Bangalore-560017, Karnataka, India
[5]Materials Research Group, Faculty of Engineering and the Environment, University of Southampton, Southampton SO17 1BJ, UK

*Corresponding author: y.huang@soton.ac.uk (Yi Huang)

Abstract

A comparative study was conducted to evaluate the influence of two different severe plastic deformation (SPD) processes: repetitive corrugation and straightening (RCS) and high-pressure torsion (HPT). Samples of an Al-3Mg-0.25Sc alloy with an initial grain size of ~150 μm were processed by RCS through 8 passes at room temperature either without any rotation during processing or with a rotation of 90° around the longitudinal axis between each pass. Thin discs of the alloy were also processed for up to 5 turns by HPT at room temperature. The results show that both procedures introduce significant grain refinement with average grain sizes of ~0.6-0.7 μm after RCS and ~95 nm after HPT. Measurements of the Vickers microhardness gave values of ~128 after RCS and ~156 after HPT. The results demonstrate that processing by HPT is the optimum processing technique in achieving both high strength and microstructural homogeneity.

***Keywords*:** Al-Mg-Sc alloy; high-pressure torsion; homogeneity; repetitive corrugation and straightening; ultrafine grains

1. Introduction

Various severe plastic deformation (SPD) techniques are now available for achieving ultrafine-grained (UFG) metals with grain sizes in the submicrometer or nanometer ranges [1]: examples of these techniques include equal-channel angular pressing (ECAP) [2], high-pressure torsion (HPT) [3], accumulative roll bonding (ARB) [4], multi-directional forging [5] and multi-axial compression (MAC) [6]. A significant advantage of SPD processing is that it involves procedures in which bulk metals are subjected to very high strains but without introducing any significant change in their overall geometries. Thus, these procedures are now attracting considerable attention because of their potential for introducing exceptional mechanical and functional properties [7-11].

Recently, much attention has focused on processing by HPT because this procedure produces grains that are exceptionally small [12,13] and the grains generally have high fractions of high-angle grain boundaries [14]. Nevertheless, a disadvantage with HPT is that the samples are usually in the form of very thin discs and there are difficulties associated with scaling the processing to involve larger cylindrical samples [15,16].

An alternative and relatively simple SPD procedure is repetitive corrugation and straightening (RCS) which was first introduced more than ten years ago [17,18], In this process, a sample in the form of a sheet is repetitively bent and straightened without significantly changing the cross-sectional geometry and thereby the process introduces a large plastic strain which leads to grain refinement. It is well established that the RCS process produces bulk nanostructured materials that are free of any contaminants or porosity. Furthermore, processing by RCS appears to be appropriate for use in large-scale industrial applications as, for example, in the production of fuselage structures in the aerospace industry. Nevertheless, to date there are only a limited number of reports describing investigations using RCS processing. Early investigations of RCS evaluated the process with pure Cu [17-19] but later experiments used pure Al and Al-0.25% Sc [20], Cu-2% Ni-1% Si [21-23], a Co superalloy [24], Cu-0.6% Cr [22,25-27], Cu-30% Zn [27], Cu-37% Zn [23], Al-4% Cu-2% Sc [28] and an AA2024 Al-Cu alloy [28].

Although processing by HPT is generally regarded as the optimum SPD process for producing exceptional grain refinement, there has been no attempt so far to make a critical comparison of the microstructures that are produced using HPT and RCS. Accordingly, the present research was initiated to provide a detailed comparison between these two SPD techniques with special emphasis on the grain sizes and the levels of homogeneity that may be achieved. In addition, hardness values were compared by taking measurements of the Vickers microhardness both across diameters of HPT discs and along the lengths of RCS samples. The experiments were conducted using an Al-3% Mg-0.25% Sc alloy where this material was selected because there are numerous experiments showing that Al-Mg-Sc alloys are easily processed by HPT [29-31] and earlier experiments demonstrated the successful processing of aluminum-based alloys by RCS [20,28].

2. Experimental material and procedures

Selected quantities of commercial purity (99.99%) aluminum, an Al-2 wt.% Sc alloy and an Al-3 wt.% Mg alloy were melted in a graphite crucible in an electrical

resistance furnace at 1073 K. The melt was then maintained at 973 K for 10 min before pouring into a metal mold to obtain an as-cast Al-3Mg-0.25 Sc alloy which was homogenized at 758 K for 24 h. In this condition, the average initial grain size determined by optical microscopy was ~150 μm which is consistent with earlier reports for cast Al-Mg-Sc alloys [32,33]. Samples were cut into blocks with dimensions of 80 × 12 × 12 mm^3 for RCS processing and rods were prepared with diameters of 10.5 mm and lengths of 90 mm for subsequent HPT processing.

For RCS, the block samples were subjected to a repetitive bending and straightening operation in which the straightening restored the initial shape. Each sample was processed through a total of eight passes at room temperature (298 K) either without any rotation during processing or with a rotation of 90° in the same sense around the longitudinal axis between each separate pass. For processing by HPT, the rods were machined to diameters of 10 mm and then sliced into discs with thicknesses of ~1 mm. These discs were polished to final thickness of ~0.85 mm and then processed using an HPT facility operating under quasi-constrained conditions [34,35] in which the disc is held under an applied pressure between two massive anvils and there is a limited outward flow of material around the periphery of the disc during processing. The HPT was conducted at room temperature under an applied pressure of 6.0 GPa with a rotational speed of 1 rpm and for different numbers of turns, N, up to a maximum of 5 turns.

The samples processed by RCS and HPT were evaluated in different ways as illustrated in Fig. 1 where the RCS sample is shown at the top and the HPT sample at the bottom. For the as-cast and RCS processed samples, the Vickers microhardness, Hv, was recorded along linear traverses on each sample using a METATEK hardness tester. These measurements were recorded along a central longitudinal line at incremental separations of 10 mm using a load of 0.5 kgf and a dwell time for each measurement of 10 s. For the HPT discs, the samples were prepared to a mirror-like condition and then Vickers hardness measurements were recorded along diameters of the samples at incremental separations of 0.5 mm using a Micro-DUROMAT4000 facility with a load of 100 g and a dwell time of 15 s. Following conventional practice [36], individual hardness values were recorded at four selected points approximately equally spaced around each point of measurement. Thus, it is apparent from Fig. 1 that the incremental spacings between the microhardness indentations were 10 and 0.5 mm for the RCS and HPT samples, respectively.

Small discs of ~3 mm diameter were prepared for transmission electron microscopy (TEM) at the positions indicated on the RCS and HPT samples in Fig. 1 where these observations were conducted near the ends of the blocks for the RCS samples and at the centers and edge positions for the HPT samples. All discs were mechanically ground and then electro-polished using a perchloric acid-ethanol mixture. The TEM observations were conducted using a JEOL JEM 2100 instrument operating at a voltage of 200 kV.

3. Experimental results

In order to evaluate the significance of microstructural inhomogeneties in samples processed by these two different SPD techniques, it is now well established that the most convenient approach is to take measurements of the local microhardness

at selected points and to undertake a series of microstructural observations using TEM [37-40]. Adopting this approach, the following section describes the results obtained using RCS processing and the next section describes the results from HPT processing.

3.1 Hardness and microstructural evolution in RCS processing

The average microhardness values recorded along the central longitudinal sections of the RCS samples are shown in Fig. 2 where the lower line denotes the initial as-cast condition and the two upper lines show measurements taken on the RCS samples after 8 passes either with or without rotation during processing. These results show that the initial hardness is Hv $\approx$ 50 but the hardness is increased to a much higher value of Hv $\approx$ 110 after RCS through 8 passes without rotation and then further increased to Hv $\approx$ 128 if the block is rotated by 90° between passes. This beneficial effect of sample rotation during SPD processing is not generally recognized in RCS but it is consistent with earlier results demonstrating the advantage of sample rotation when processing using ECAP [41,42]. An important conclusion from Fig. 2 is that RCS leads both to high hardness and, more importantly, to hardness values that are essentially uniform throughout the length of the sample

A representative TEM micrograph is shown in Fig. 3 for the RCS sample processed through 8 passes without rotation together with the corresponding selected area electron diffraction (SAED) pattern. Detailed measurements showed that processing by RCS produced very substantial grain refinement with average grain sizes of ~0.7 μm when processing without rotation. Measurements suggested a slightly smaller grain size of ~0.6 μm when using rotation between each pass. As noted in Fig. 3, there was a tendency for the presence of some elongated grains and a high dislocation density when processing without rotation. In general, all observations showed that the grain boundaries after RCS were wavy and diffuse and this matches earlier reports for materials processed by ECAP [43,44]. It is well established that this corresponds to the introduction of non-equilibrium boundaries having high energies and an excess of extrinsic dislocations [45,46].

3.2 Hardness and microstructural evolution in HPT processing

Processing by HPT produces a very significant strengthening as shown by the microhardness measurements recorded in Fig. 4: again, the lower line denotes the as-cast material at Hv $\approx$ 50 and the upper lines depict the recorded hardness values obtained at incremental spacings of 0.5 mm for samples processed through 1/2 to 5 turns.

Two significant conclusions may be reached from inspection of the data in Fig. 4. First, the hardness values are initially low near the centre of the disc and high at the edge but gradually the values increase near the center until ultimately, after 5 turns, the hardness values are fairly uniform across the disc diameter with Hv $\approx$ 150-156. During this straining, the hardness remains reasonably constant at the edge of the disc but increases substantially in the central region. This evolution towards a uniform distribution of hardness values is consistent with theoretical predictions for HPT processing based on strain gradient plasticity modeling [47]. The tendency for lower hardness values to occur initially in the centres of the discs is consistent with many earlier reports for several different materials including Al [48] and Cu [49] alloys and the

gradual evolution towards a saturation hardness is also well documented in many metals [50-52]. Thus, the present results show that a reasonable level of homogeneity is achieved after 5 turns of HPT. Second, the final hardness after 5 turns is Hv ≥ 150 and, by considering Fig. 2, this value is significantly higher than the maximum hardness achieved in RCS processing after 8 passes with rotation of the sample after every pass. Therefore, these results confirm the advantage of processing by HPT by comparison with RCS.

A representative TEM micrograph and SAED pattern is shown in Fig. 5 recorded at the edge of the disc after processing through only 1 turn. For this condition, the observations showed arrays of ultrafine grains with a measured average size of ~95 nm. The SAED pattern in Fig. 5 indicates the presence of many small grains having multiple orientations within the field of view and with the boundaries having high angles of misorientation. It is readily apparent by inspection of Fig. 4 that the condition in Fig. 5 is very close to the saturation condition for this alloy since the edge region saturates in the very early stages of HPT processing. In general, the microstructure in the central region appeared to be coarser with an ill-defined microstructure containing many low-angle subgrain boundaries. These results are generally typical of Al-Mg alloys processed by HPT through small numbers of turns [53].

4. Discussion

An Al-3Mg-0.25Sc alloy with an initial grain size of ~150 μm was processed by two different SPD techniques: RCS in which a block of material is continuously corrugated and straightened and HPT in which a thin disc is subjected to a high applied pressure and concurrent torsional straining. The results show that both of these SPD procedures give significant grain refinement but the final grain sizes are different. In RCS it is possible to produce a grain size of ~0.6 μm by processing through 8 passes provided the material is rotated in a longitudinal sense by 90° between each pass. In HPT the final grain size is much smaller at ~95 nm. Thus, HPT processing is recognized as the optimum procedure for achieving the maximum grain refinement. The smaller grains attained by HPT are consistent with an earlier investigation comparing MAC and HPT where the final grain sizes in an Al-4Cu alloy were ~0.5 μm after processing by MAC through 35 passes at a temperature of 373 K and this contrasted with a grain size of ~0.25 μm after processing by HPT through 5 turns at room temperature [6].

In the present investigation, both RCS and HPT produce a reasonable level of homogeneity but the microstructures after HPT processing were generally more uniform. Thus, processing by HPT produced an array of ultrafine equiaxed grains whereas processing by RCS produced grain refinement but with the presence of some elongated grains in the absence of any sample rotation as shown in Fig. 3. The favourable characteristics of HPT processing by comparison with RCS is attributed to the presence of near uniform simple shear throughout the HPT processing which contrasts with the unsteady and irregular deformation imposed when processing by RCS. It should be noted that the microhardness results documented in Figs 2 and 4 are consistent with the observed microstructures. Thus, the grain size is smaller in HPT and this leads, in the saturation condition, to hardness values that are significantly higher in HPT than in RCS.

Despite the clear advantage in processing by HPT, it is important to note that the samples used in HPT processing are generally very small and typically in the form of discs having thicknesses of <1.0 mm. This places an overall limitation on the utilization of samples from HPT processing whereas in RCS processing it is feasible to make use of relatively large samples. Furthermore, the hardness values recorded in Fig. 2 for RCS processing, although lower than the values in Fig. 4 for HPT processing, nevertheless show excellent uniformity over the total length of the sample corresponding to a total length of ~80 mm in this investigation. It is reasonable to anticipate that this uniformity will be achieved even when processing much longer sheets.

There have been recent new developments in HPT in attempts to overcome the size limitation which is an inherent feature of this processing method. For example, HPT has been undertaken with small cylindrical samples [15] and continuous processing has been introduced using either strip [54] or wire [55] samples. Alternatively, the recent introduction of incremental HPT provides the opportunity to make use of samples having much larger aspect ratios [56]. It appears that all of these approaches have the potential for significantly increasing the overall viability of the HPT processing method.

5. Summary and conclusions

[1]   Experiments were conducted on an Al-3Mg-0.25Sc alloy to provide a direct comparison between two different SPD processing procedures: repetitive corrugation and straightening (RCS) and high pressure torsion (HPT). The grain size of the alloy in the initial condition was ~150 μm and the hardness was Hv $\approx$ 50.

[2]   The experimental results show that processing by RCS through 8 passes at room temperature produces significant grain refinement with measured average grain sizes of ~0.7 µm when processing without rotation and ~0.6 µm when rotating the sample by 90° in the same sense between each pass. Measurements of the Vickers microhardness after RCS processing showed that the hardness values remained constant along the total length of the sample with values of Hv $\approx$ 110 when processing without rotation and Hv $\approx$ 128 when processing with rotation. There was evidence for some elongated grains in the materials processed by RCS without rotation.

[3]   Processing by HPT through one turn at room temperature using a pressure of 6.0 GPa produced a reasonably homogeneous microstructure with equiaxed ultrafine grains having an average size of ~95 nm. As in conventional HPT, the hardness increased rapidly around the periphery of the disc during HPT but the hardness in the central region increased more slowly. There was good microhardness homogeneity throughout the disc after processing through 5 turns with an average hardness of Hv $\approx$ 150-156.

[4]   The results demonstrate that processing by HPT produces a smaller grain size, higher values for the Vickers microhardness and a more homogeneous microstructure than processing by RCS.

Acknowledgement

References

[1]   Valiev RZ, Estrin Y, Horita Z, Langdon TG, Zehetbauer MJ, Zhu YT. Producing bulk ultrafine-grained materials by severe plastic deformation. JOM 2006;58(4):33-39.

[2]   Valiev RZ, Langdon TG. Principles of equal-channel angular pressing as a processing tool for grain refinement. Prog. Mater. Sci. 2006;51:881-981.

[3]   Zhilyaev AP, Langdon TG. Using high-pressure torsion for metal processing: Fundamentals and applications. Prog. Mater. Sci. 2008;53:893-979.

[4]   Saito Y, Tsuji N, Utsunomiya H, Sakai T, Hong RG. Ultra-fine grained bulk aluminum produced by accumulative roll-bonding (ARB) process. Scr. Mater. 1998;39:1221-1227.

[5]   Salishchev GA, Zherebtsov SV, Mironov SYu, Myshlayev MM, Pippan R, in: Zehetbauer MJ, Valiev RZ (Eds.), Nanomaterials by Severe Plastic Deformation, Wiley-VCH, Weinheim, Germany, 2004, p. 691.

[6]   Xu XC, Zhang Q, Hu N, Huang Y, Langdon TG. Using an Al–Cu binary alloy to compare processing by multi-axial compression and high-pressure torsion. Mater. Sci. Eng. A 2013;588:280-287.

[7]   Valiev RZ, Langdon TG. The art and science of tailoring materials by nanostructuring for advanced properties using SPD techniques. Adv. Eng. Mater. 2010;12:677-691.

[8]   Estrin Y, Vinogradov A. Extreme grain refinement by severe plastic deformation: A wealth of challenging science. Acta Mater. 2013;61:782-817.

[9]   Langdon TG. Twenty-five years of ultrafine-grained materials: Achieving exceptional properties through grain refinement. Acta Mater. 2013;61:7035-7059.

[10] Valiev RZ. Superior strength in ultrafine-grained materials produced by SPD processing. Mater. Trans. 2014;55:13-18.

[11] Valiev RZ, Estrin Y, Horita Z, Langdon TG, Zehetbauer MJ, Zhu YT. Fundamentals of superior properties in bulk NanoSPD materials. Mater. Res. Lett. 2016; DOI: 10.1080/21663831.2015.1060543.

[12] Zhilyaev AP, Lee S, Nurislamova GV, Valiev RZ, Langdon TG. Microhardness and microstructural evolution in pure nickel during high-pressure torsion. Scr. Mater. 2001;44:2753-2758.

[13] Zhilyaev AP, Nurislamova GV, Kim BK, Baró MD, Szpunar JA, Langdon TG. Experimental parameters influencing grain refinement and microstructural evolution during high-pressure torsion. Acta Mater. 2003;51:753-765.

[14] Wongsa-Ngam J, Kawasaki M, Langdon TG. A comparison of microstructures and mechanical properties in a Cu–Zr alloy processed using different SPD techniques, J. Mater. Sci. 2013;48:4653-4660.

[15] Sakai G, Nakamura K, Horita Z, Langdon TG. Developing high-pressure torsion for use with bulk samples. Mater. Sci. Eng. A 2005;406:268-273.

[16] Hohenwarter A, Bachmaier A, Gludovatz B, Scheriau S, Pippan R. Technical parameters affecting grain refinement by high pressure torsion. Int. J. Mater. Res. 2009;100:1653-1661.

[17] Zhu YT, Jiang HG, Huang JY, Lowe TC. A new route to bulk nanostructured metals. Metall. Mater. Trans. A 2001;32:1559-1562.

[18] Huang JY, Zhu YT, Jiang HG, Lowe TC. Microstructures and dislocation configurations in nanostructured Cu processed by repetitive corrugation and straightening. Acta Mater. 2001;49:1497-1501.

[19] Huang JY, Zhu YT, Alexander DJ, Liao XZ, Lowe TC, Asaro RJ. Development of repetitive corrugation and straightening. Mater. Sci. Eng. A 2004;371:35-39.

[20] Rajinikanth V, Arora G, Narasaiah N, Venkateswarlu K. Effect of repetitive corrugation and straightening on Al and Al-0.25Sc alloy. Mater. Lett. 2008;62:301-304.

[21] Stobrawa J, Rdzawski Z, Gluchowski W, Malec W. Microstructure and properties of CuNi2Si1 alloy processed by continuous RCS method, J. Achiev. Mater. Manuf. Eng. 2009;37:466-479.

[22] Stobrawa J, Rdzawski Z, Gluchowski W, Malec W. Ultrafine grained strips of precipitation hardened copper alloys. Archiv. Metall. Mater. 2011;56:171-179.

[23] Gluchowski W, Stobrawa J, Rdzawski Z, Malec W. Ultrafine grained copper alloys processed by continuous repetitive corrugation and straightening method. Mater. Sci. Forum 2011;674:177-188.

[24] Sheikh H, Paimozd E, Hashemi SM. Work hardening of Duratherm 600 cobalt superalloy using repetitive corrugation and straightening process. Russ. J. Non-Ferr. Met. 2010;51:59-61.

[25] Stobrawa J, Rdzawski Z, Gluchowski W, Malec W. Ultrafine grained strips of CuCr0.6 alloy prepared by CRCS method. J. Achiev. Mater. Manuf. Eng. 2009;33:166-172.

[26] Stobrawa JP, Rdzawski ZM, Gluchowski W, W. Malec W. Microstructure evolution in CRCS processed strips of CuCr0.6 alloy, J. Achiev. Mater. Manuf. Eng. 2010;38:195-202.

[27] Gluchowski W, Stobrawa JP, Rdzawski ZM. Microstructure refinement of selected copper alloys strips processed by SPD method, Arch. Mater. Sci. Eng. 2011;47:103-109.

[28] Pandey SC, Joseph MA, Pradeep MS, Ragahavendra K, Ranganath VR, Venkateswarlu K, Langdon TG. A theoretical and experimental evaluation of repetitive corrugation and straightening: Application to Al-Cu and Al-Cu-Sc alloys, Mater. Sci. Eng. A 2012;534:282-287.

[29] Sakai G, Horita Z, Langdon TG. Grain refinement and superplasticity in an aluminum alloy processed by high-pressure torsion. Mater. Sci. Eng. A 2005;393:344-351.

[30] Horita Z, Langdon TG. Microstructures and microhardness of an aluminum alloy and pure copper after processing by high-pressure torsion. Mater. Sci. Eng. A 2005;410-411:422-425.

[31] Horita Z, Langdon TG. Achieving exceptional superplasticity in a bulk aluminum alloy processed by high-pressure torsion. Scr. Mater. 2008;58:1029-1032.

[32] Komura S, Furukawa M, Horita Z, Nemoto M, Langdon TG. Optimizing the procedure of equal-channel angular pressing for maximum superplasticity. Mater. Sci. Eng. A 2001;297:111-118.

[33] Horita Z, Furukawa M, Nemoto M, Barnes AJ, Langdon TG. Superplastic forming at high strain rates after severe plastic deformation. Acta Mater. 2000;48:3633-3640.

[34] Figueiredo RB, Cetlin PR, Langdon TG. Using finite element modeling to examine the flow processes in quasi-constrained high-pressure torsion. Mater. Sci. Eng. A 2011;528:8198-8204.

[35] Figueiredo RB, Pereira PHR, Aguilar MTP, Cetlin PR, Langdon TG. Using finite element modeling to examine the temperature distribution in quasi-constrained high-pressure torsion. Acta Mater. 2012;60:3190-3198.

[36] Kawasaki M, Langdon TG. The significance of strain reversals during processing by high-pressure torsion. Mater. Sci. Eng. A 2008;498:341-348.

[37] Xu C, Horita Z, Langdon TG. The evolution of homogeneity in processing by high-pressure torsion. Acta Mater. 2007;55:203-212.

[38] Xu C, Horita Z, Langdon TG. The evolution of homogeneity in an aluminum alloy processed using high-pressure torsion. Acta Mater. 2008;56:5168-5176.

[39] Kawasaki M, Horita Z, Langdon TG. Microstructural evolution in high purity aluminum processed by ECAP. Mater. Sci. Eng. A 2009;524:143-150.

[40] Xu C, Horita Z, Langdon TG. Microstructural evolution in an aluminum solid solution alloy processed by ECAP. Mater. Sci. Eng. A 2011;528:6059-6065.

[41] Iwahashi Y, Horita Z, Nemoto M, Langdon TG. An investigation of microstructural evolution during equal-channel angular pressing. Acta Mater. 1997;45:4733-4741.

[42] Iwahashi Y, Horita Z, Nemoto M, Langdon TG. The process of grain refinement in equal-channel angular pressing, Acta Mater. 1998;46:3317-3331.

[43] Wang J, Horita Z, Furukawa M, Nemoto M, Tsenev NK, Valiev RZ, Ma Y, Langdon TG. An investigation of ductility and microstructural evolution in an al-3-percent mg alloy with submicron grain-size. J. Mater. Res. 1993;8:2810-2818.

[44] Wang J, Iwahashi Y, Horita Z, Furukawa M, Nemoto M, Valiev RZ, Langdon TG. An investigation of microstructural stability in an Al-Mg alloy with submicrometer grain size. Acta Mater. 1996;44:2973-2982.

[45] Valiev RZ, Musalimov RSh, Tsenev NK. The non-equilibrium state of grain-boundaries and the grain-boundary precipitations in aluminum-alloys. Phys. Stat. Solidi (a) 1989;115:451-457.

[46] Nazarov AA, Romanov AE, Valiev RZ. On the structure, stress-fields and energy of nonequilibrium grain-boundaries. Acta Metall. Mater. 1993;41:1033-1040.

[47] Estrin Y, Molotnikov A, Davies CHJ, Lapovok R. Strain gradient plasticity modelling of high-pressure torsion. J. Mech. Phys. Solids 2008;56:1186-1202.

[48] Sabbaghianrad S, Kawasaki M, Langdon TG. Microstructural evolution and the mechanical properties of an aluminum alloy processed by high-pressure torsion, J. Mater. Sci. 2012;47:7789-7795.

[49] Wongsa-Ngam J, Kawasaki M, Langdon TG. Achieving homogeneity in a Cu–Zr alloy processed by high-pressure torsion. J. Mater. Sci. 2012;47:7782-7788.

[50] Vorhauer A, Pippan R. On the homogeneity of deformation by high pressure torsion. Scr. Mater. 2004;51:921-925.

[51] Kawasaki M. Different models of hardness evolution in ultrafine-grained materials processed by high-pressure torsion. J. Mater. Sci. 2014;49:18-34.

[52] Sabbaghianrad S, Langdon TG. An evaluation of the saturation hardness in an ultrafine-grained aluminum 7075 alloy processed using different techniques. J. Mater. Sci. 2015;50:4357-4365.

[53] Bazarnik P, Huang Y, Lewandowska M, Langdon TG. Structural impact on the Hall–Petch relationship in an Al–5Mg alloy processed by high-pressure torsion. Mater. Sci. Eng. A 2015;626:9-15.

[54] Edalati K, Horita Z. Continuous high-pressure torsion. J. Mater. Sci. 2010;45:4578-4582.

[55] Edalati K, Lee S, Horita Z. Continuous high-pressure torsion using wires. J. Mater. Sci. 2012;47:473-478.

[56] Hohenwarter A. Incremental high pressure torsion as a novel severe plastic deformation process: Processing features and application to copper. Mater. Sci. Eng. A 2015;626:80-85.

Figure captions

Fig. 1 Schematic illustrations of the hardness measurement points and the positions for the TEM samples for the RCS (upper) and HPT (lower) samples.

Fig. 2 Values of the Vickers microhardness for the as-cast alloy and the alloy processed by 8 passes of RCS with and without rotation plotted against the distance measured on the samples in a longitudinal direction.

Fig. 3 TEM image showing representative microstructure and SAED pattern after processing by RCS for 8 passes without rotation.

Fig. 4 Values of the Vickers microhardness for the as-cast alloy and the alloy processed by HPT through up to a maximum of 5 turns plotted against the distance from the centre of each disc.

Fig. 5 TEM image showing representative microstructure and SAED pattern after processing by HPT for 1 turn in the edge region of the disc.
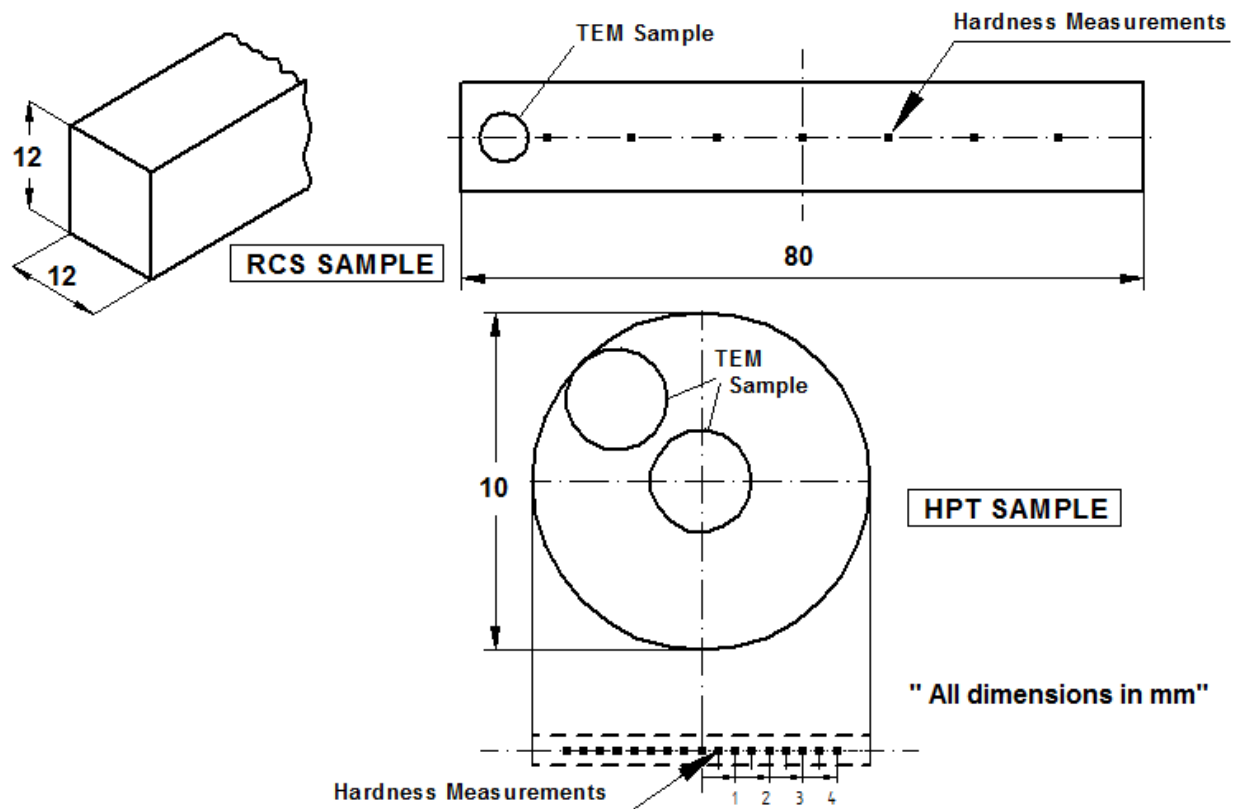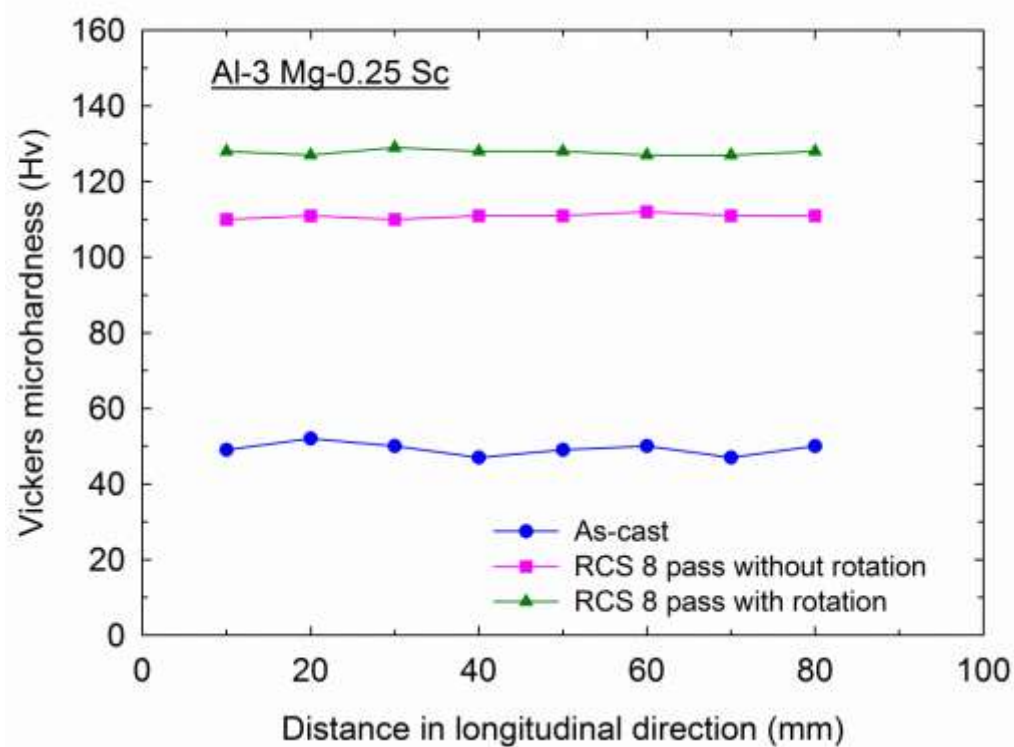
Figure 1 Schematic illustrations of the hardness measurement points and the positions for the TEM samples for the RCS (upper) and HPT (lower) samples.

Figure 2 Values of the Vickers microhardness for the as-cast alloy and the alloy processed by 8 passes of RCS with and without rotation plotted against the distance measured on the samples in a longitudinal direction.
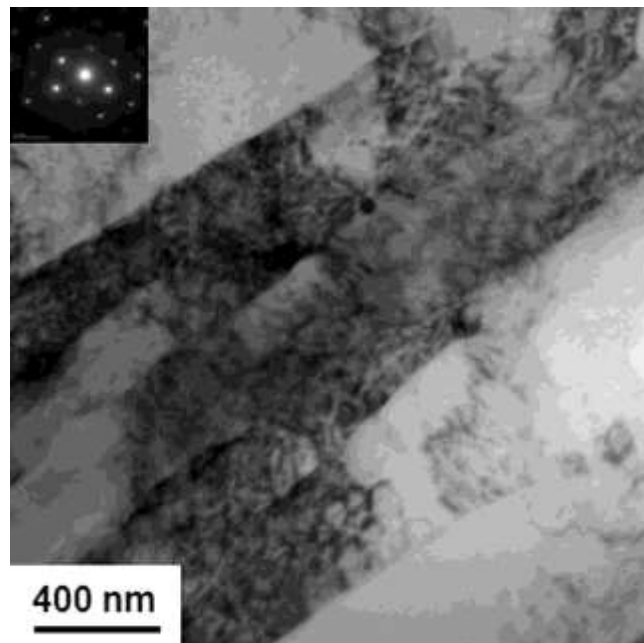
Figure 3 TEM image showing representative microstructure and SAED pattern after processing by RCS for 8 passes without rotation.
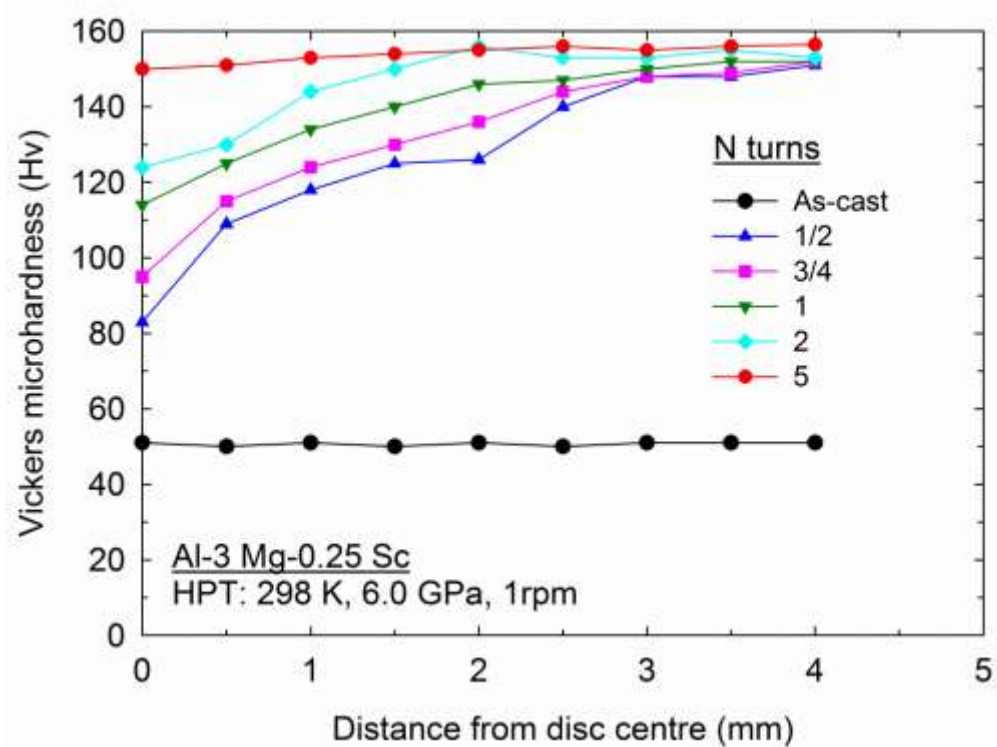
Figure 4 Values of the Vickers microhardness for the as-cast alloy and the alloy processed by HPT through up to a maximum of 5 turns plotted against the distance from the centre of each disc.
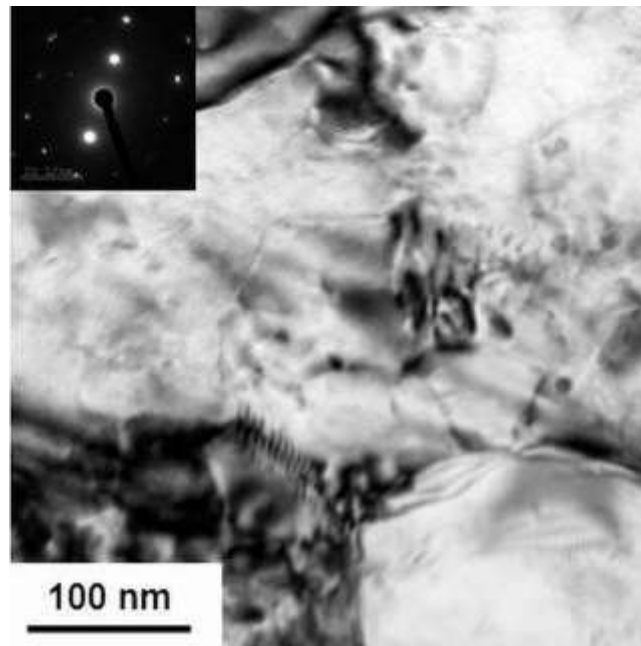
Figure 5 TEM image showing representative microstructure and SAED pattern after processing by HPT for 1 turn in the edge region of the disc.